

Neutral-depletion-induced axially asymmetric density in a helicon source and imparted thrust

Kazunori Takahashi, Yoshinori Takao, and Akira Ando

Citation: [Applied Physics Letters](#) **108**, 074103 (2016); doi: 10.1063/1.4942469

View online: <http://dx.doi.org/10.1063/1.4942469>

View Table of Contents: <http://scitation.aip.org/content/aip/journal/apl/108/7?ver=pdfcov>

Published by the [AIP Publishing](#)

Articles you may be interested in

[Neutral depletion and the helicon density limit](#)

Phys. Plasmas **20**, 123511 (2013); 10.1063/1.4849376

[Reduction of plasma density in the Helicity Injected Torus with Steady Inductance experiment by using a helicon pre-ionization source](#)

Rev. Sci. Instrum. **84**, 103506 (2013); 10.1063/1.4824707

[Evidence of current free double layer in high density helicon discharge](#)

Phys. Plasmas **20**, 013510 (2013); 10.1063/1.4789455

[The study of helicon plasma sourcea\)](#)

Rev. Sci. Instrum. **81**, 02B105 (2010); 10.1063/1.3271172

[Experimental Measurements and Modeling of a Helicon Plasma Source with Large Axial Density Gradients](#)

AIP Conf. Proc. **694**, 427 (2003); 10.1063/1.1638072

The image shows the cover of an Applied Physics Reviews journal. It features a blue and orange color scheme with a molecular structure background. The text 'NEW Special Topic Sections' is prominently displayed in white. Below it, 'NOW ONLINE' is written in yellow, followed by the title 'Lithium Niobate Properties and Applications: Reviews of Emerging Trends' in white. The AIP Applied Physics Reviews logo is in the bottom right corner.

NEW Special Topic Sections

NOW ONLINE
Lithium Niobate Properties and Applications:
Reviews of Emerging Trends

AIP Applied Physics
Reviews

Neutral-depletion-induced axially asymmetric density in a helicon source and imparted thrust

Kazunori Takahashi,^{1,a)} Yoshinori Takao,² and Akira Ando¹

¹Department of Electrical Engineering, Tohoku University, Sendai 980-8579, Japan

²Division of Systems Research, Yokohama National University, Yokohama 240-8501, Japan

(Received 14 December 2015; accepted 9 February 2016; published online 18 February 2016)

The high plasma density downstream of the source is observed to be sustained only for a few hundreds of microsecond at the initial phase of the discharge, when pulsing the radiofrequency power of a helicon plasma thruster. Measured relative density of argon neutrals inside the source implies that the neutrals are significantly depleted there. A position giving a maximum plasma density temporally moves to the upstream side of the source due to the neutral depletion and then the exhausted plasma density significantly decreases. The direct thrust measurement demonstrates that the higher thrust-to-power ratio is obtained by using only the initial phase of the high density plasma, compared with the steady-state operation. © 2016 AIP Publishing LLC.
[\[http://dx.doi.org/10.1063/1.4942469\]](http://dx.doi.org/10.1063/1.4942469)

Plasma production and expansion in an expanding magnetic field have been investigated in association with space plasmas, plasma processing, and electrodeless electric propulsion devices.¹ A number of laboratory experiments have been conducted to investigate underlying physics and to test a propulsion device called a helicon plasma thruster (HPT).^{1–3} A high density plasma produced by a helicon source is transported along the external magnetic field and expands along the magnetic nozzle, by which the plasma is accelerated into the axial direction. Hence, the typical HPT consists of only an insulator source cavity wound by a radio-frequency (rf) antenna, solenoids or permanent magnets providing an external magnetic field, and a gas injector located upstream of the source cavity. One of the key parameters of the thruster is a plasma momentum exhausted from the system, which corresponds to the thrust imparted by the thruster. Direct measurement of the thrust has recently been performed by using thrust balances.^{3–6} Some experiments have also been conducted to improve the thruster performance.^{7,8} The plasma momentum is also the essential parameter relating to particle acceleration in space, thermonuclear fusion, and laboratory plasmas; the direct thrust measurement is equivalent to identification of the absolute value of the momentum and gives important insight into the plasma transport and expansion physics.

The static magnetic field has two roles in the HPT operation. One is the magnetic nozzle effect in the plasma expansion. One of the authors have demonstrated the presence of the thrust component arising from the magnetic nozzle,⁹ where the radial component of the plasma momentum is converted into the axial one via a Lorentz force arising from the radial magnetic field and an azimuthal plasma current.^{10,11} The other role is production of a high density plasma via a helicon-wave absorption and a radial plasma confinement, thereby providing a plasma density in the range of 10^{12} – 10^{13} cm⁻³.¹² In the highly ionized state, a number of experiments have shown neutral depletion phenomena in

steady-state plasmas.^{13–18} One of the early experiments has observed the oscillation of the plasma density due to the neutral depletion.¹⁹ In a high-power electron cyclotron resonance plasma, a vortex structure has also been driven by the depleted neutrals.²⁰ As mentioned above, the neutral-plasma interactions significantly affect both the steady-state and spatiotemporal plasma characteristics.

Fruchtman *et al.* have predicted by using a non-magnetic field model that an axially asymmetric plasma density profile in steady state is formed due to the neutral depletion when introducing the gas from one end of the source.^{21,22} Similar profiles have also been reported in a two-dimensional model of the HPT²³ and have recently observed in the HPT experiment when changing a propellant gas from Ar to Kr or Xe,²⁴ although no experimental evidence of the neutral depletion has been shown. Simultaneously with the formation of the asymmetric density profile, non-negligible axial momentum lost to the radial wall has been detected.²⁴ The loss of the axial momentum to the radial wall is considered to occur when the ions accelerated by an electric field in the plasma core are lost to the radial wall. Such a physical picture has also been validated by a particle-in-cell simulation with no magnetic field.²⁵ Although the discrepancies between the models and experiments such as the presence of the magnetic field are still found, there seems to be a universal physics relating to the neutral depletion. Here, a spatio-temporal evolution reaching the axially asymmetric profile of the plasma density due to the neutral depletion is demonstrated; it is found that the high plasma density downstream of the source is sustained only for the initial phase of the discharge. Furthermore, the thrust-to-power ratio is improved by utilizing only the high density initial phase, which also indicates the decrease in the thrust due to the neutral depletion.

Figure 1 shows a schematic of the HPT attached to a pendulum thrust balance⁸ immersed in a 1-m-diameter and 2-m-long cylindrical vacuum chamber, which is evacuated to a base pressure of 1×10^{-6} Torr by a turbomolecular/rotary pumping system. The HPT has a 6.5-cm-inner

^{a)}kazunori@ecei.tohoku.ac.jp

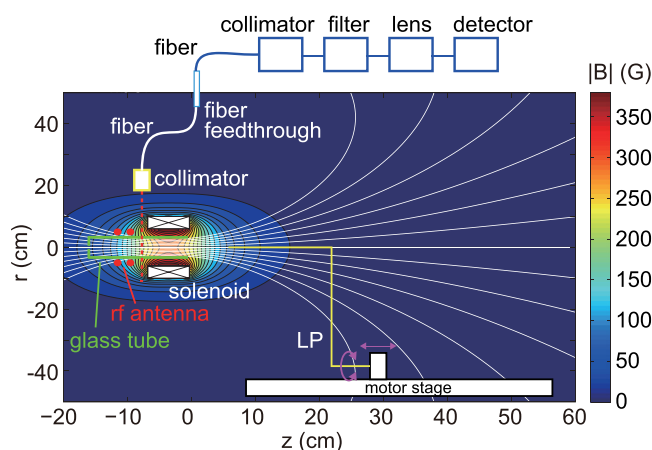
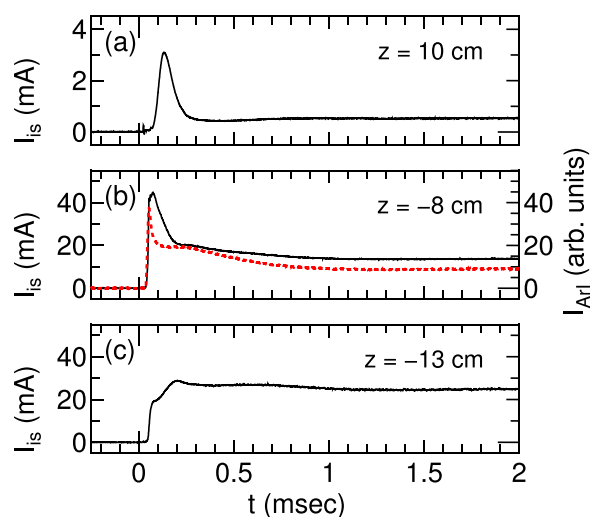


FIG. 1. Schematic diagram of the HPT setup.

diameter and 16-cm-long source cavity consisting of a pyrex tube and an insulator back plate, a double-turn rf loop antenna located around $z = -10.5 \pm 1$ cm, and a solenoid located at $z = -1$ cm, where $z = 0$ is defined as the downstream edge of the solenoid holder. The antenna is shielded to suppress parasitic and anomalous discharges outside of the source;²⁶ the location of the antenna is chosen as this position due to the mechanical structure. A dc current of 4.5 A is supplied to the solenoid, and the calculated magnetic field lines and strength are shown in Fig. 1 by solid lines and a contour plot, respectively. Argon gas is continuously introduced from the back plate with a flow rate of 70 sccm giving a chamber pressure of ~ 0.6 mTorr. The rf antenna is powered from a 13.56 MHz rf generator and pulsed with a repetition frequency of 200 Hz. The instantaneous power can be increased up to $P_{rf} = 5$ kW, where the duty ratio is changeable in the range of $D_R = 3\% - 100\%$ and the averaged rf power is defined as $\langle P_{rf} \rangle \equiv P_{rf} D_R$.

A radially facing and cat-leg planar Langmuir probe (LP) is mounted on a motor stage immersed in vacuum. The temporal evolution of the ion saturation current I_{is} is measured with the probe bias voltage of -70 V. When assuming a constant electron temperature, I_{is} is proportional to the plasma density. An optical emission from argon neutrals is measured by using a combination of a photodetector (maximum response frequency of 10 MHz) and an optical band-pass filter (750 ± 5 nm), where an optical collimator is located inside the chamber to detect the radial line intensity at $z = -8$ cm. Since the detected emission intensity I_{ArI} is proportional to the product of the electron density (or plasma density) and the neutral density when assuming a constant electron temperature, the temporal evolution of the relative neutral density N_{Ar} is estimated by $N_{Ar} = I_{is}/I_{ArI}$. Here, the major collisional and radiative processes of the excited argon are assumed to be the electron impact excitation and the radiative light emission, as already used in previous experiments.^{27,28}

Typically measured temporal evolutions of I_{is} at $z = 10$, -8 , and -13 cm are plotted by solid lines in Figs. 2(a)–2(c), respectively, where the signals are averaged by shots and the conditions of $P_{rf} = 5$ kW and $D_R = 50\%$ ($\langle P_{rf} \rangle = 2.5$ kW and the pulsewidth of 2.5 ms) are chosen. I_{ArI} taken at $z = -8$ cm

FIG. 2. Temporal evolutions of I_{is} measured at (a) $z = 10$ cm, (b) $z = -8$ cm, and (c) $z = -13$ cm for $P_{rf} = 5$ kW and $D_R = 50\%$. The dashed line in Fig. 2(b) shows the signal I_{ArI} from the photodetector measured at $z = -8$ cm.

is also plotted by a dotted line in Fig. 2(b). The I_{is} signal in Fig. 2(a) indicates that the high plasma density exhausted from the source is sustained only for 100–200 μ s, where the rising time of the rf generator is less than a few tens of μ s and the antenna current is confirmed to be fairly constant during the pulse, i.e., no overshoot of the rf power is observed. It is found that the steady-state value of I_{is} is $\sim 15\%$ of the maximum value, which indicates the significant decrease in the plasma density exhausted from the source for $t > 0.3$ ms. The similar temporal peak of I_{is} at the initial phase is also seen in Fig. 2(b) at the earlier time compared with Fig. 2(a); hence, the high density plasma produced at the initial phase in Fig. 2(b) is considered to flow out and be detected downstream with the delay time of ~ 70 μ s as shown in Fig. 2(a). On the other hand, a very different feature is observed at $z = -13$ cm as shown in Fig. 2(c), where the value of I_{is} at the initial phase ($t < 0.2$ ms) is smaller than that in the steady-state one. These data imply that the axial profile of the plasma density temporally varies (will be shown more clearly later). I_{ArI} in Fig. 2(b) shows the temporal peak at the initial phase of the discharge and rapidly decreases, where the decay time of I_{ArI} is shorter than that of I_{is} taken at the same position. It should be mentioned that the “normalized” radial profile of I_{is} (not shown here) is confirmed to be temporally unchanged over the time in Fig. 2. In such a situation, the neutral density estimation by $N_{Ar} = I_{ArI}/I_{is}$ is valid. To avoid the division by zero value, the analyses are performed from the time when the I_{is} value reaches 10% of the temporal peak.

Figure 3(a) shows the temporal evolution of N_{Ar} for various instantaneous rf power P_{rf} for $D_R = 50\%$ and the pulsewidth of 2.5 ms. It is found that the initial maximum values of N_{Ar} are very similar with the error of $\pm 6\%$ even in the different rf power. This fact seems to validate the present procedure of the relative neutral density estimation, since the neutral density before the high density discharge is dominated by only the local gas pressure with the continuous gas injection. Simultaneously with the high density plasma

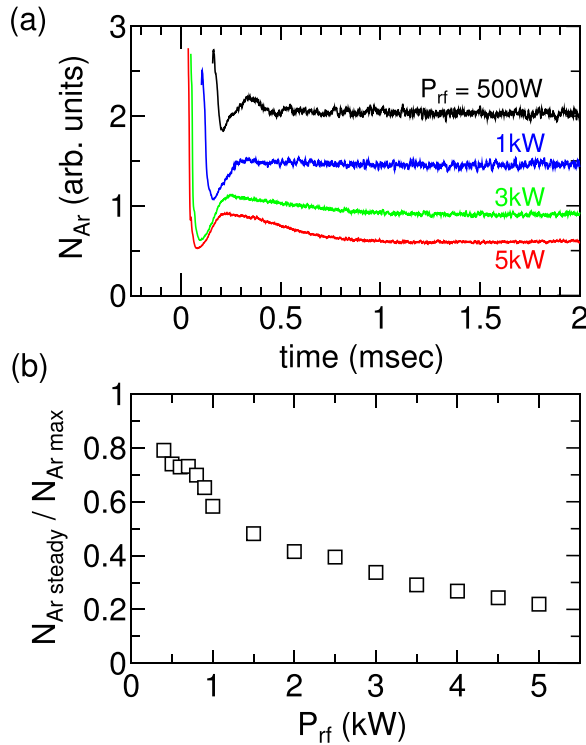


FIG. 3. (a) Temporal evolution of the relative neutral density N_{Ar} estimated from I_{Ar} and I_{is} for various rf powers P_{rf} . (b) Steady-state argon neutral density ($N_{Ar, steady}$) normalized by the maximum neutral density ($N_{Ar, max}$) at $z = -8$ cm as a function of P_{rf} at $z = -8$ cm.

production, the relative neutral density decreases with the much shorter time scale than that of I_{is} . Since the decay time is also much shorter than the transit time of both the argon neutrals and ions in the source and very close to the rising time of the plasma density [see Fig. 2(b)], it can be deduced that the decrease in the relative neutral density is caused by the local ionization process. Figure 3(b) shows the ratio of the steady-state neutral density to the initial maximum value, as a function of the instantaneous rf power P_{rf} . The relative neutral density decreases with the increase in P_{rf} and reduced to $\sim 20\%$ of the initial value at $z = -8$ cm for $P_{rf} = 5$ kW.

For such a condition of the neutral depletion, the detailed axial measurement of I_{is} is performed. Figure 4(a) shows the temporal and axial evolutions for $P_{rf} = 5$ kW, $\langle P_{rf} \rangle = 2.5$ kW, $D_R = 50\%$, and the pulsewidth of 2.5 ms. For more clarity, the axial profiles at the representative times [solid arrows in Fig. 4(a)] are plotted in Fig. 4(b). Around $t \sim 50$ – 100 μ s, the plasma density has a maximum value around $z \sim -7$ cm in the axial profile. The axial location of the maximum plasma density temporally moves to the upstream side of the source tube and is consistent with the steady-state profile predicted in Ref. 22. Therefore, the present experiment demonstrates that the neutral depletion induces the axially asymmetric density profile and then the plasma density exhausted from the source is significantly decreased. The recent experiment has shown the enhanced loss of the axial momentum to the radial wall for the asymmetric profile.²⁴ When the maximum density position exists at the upstream side of the source tube, therefore, the ions produced there have to travel longer distance to be exhausted from the source and seem to be lost to the radial wall during

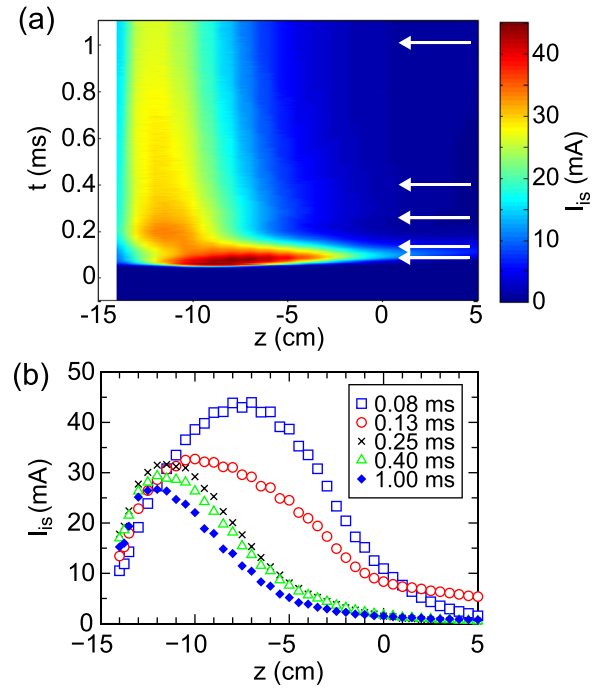


FIG. 4. (a) Temporal evolution of the axial profile of I_{is} . (b) Axial profiles of I_{is} at the representative times shown by the solid arrows in Fig. 4(a).

the transport. The ionization rate would also be changed by the neutral depletion as predicted in the models.²² Hence, these two effects of the plasma loss to the wall and the ionization rate seem to be superimposed. It should be further mentioned that the rf-power absorption profile is also affected by the antenna location and structure. Identification of the spatial profile of the rf field and its optimization remain further experimental issues to understand the relevant physics and to control the plasma density profile.

The time-averaged thrust imparted by the pulsed HPT is measured by the pendulum thrust balance, where the steady-state displacement is measured by a laser sensor. It should be mentioned that the repetition frequency (200 Hz) of the rf pulse is much higher than the oscillation frequency of the pendulum (~ 1 Hz), which allows us to measure the time-averaged thrust.²⁹ The solenoid current is now increased to 10 A to have larger thrust and the resultantly improved

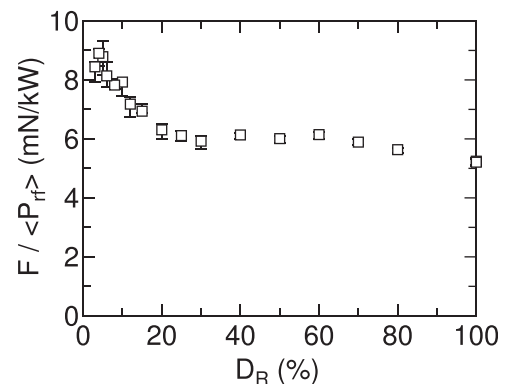


FIG. 5. Thrust-to-power ratio $F / \langle P_{rf} \rangle$ as a function of the duty ratio D_R , where the instantaneous rf power is maintained at $P_{rf} = 5$ kW and the solenoid current is chosen as 10 A.

signal-to-noise ratio in the thrust measurement. Due to the chamber maintenance and improvement, two additional turbomolecular pumps are added to the chamber; the gas pressure is decreased to about 0.2 mTorr for the same gas flow rate. The phenomena shown in Figs. 2–4 are confirmed to be essentially unchanged by the solenoid current and the pumping systems. The thrust-to-power ratio can be estimated from the measured time-averaged thrust F and the averaged rf power $\langle P_{rf} \rangle$ as $F/\langle P_{rf} \rangle = F/(P_{rf}D_R)$ and plotted in Fig. 5 as a function of the duty ratio D_R , where the instantaneous power is maintained at $P_{rf} = 5$ kW and only the pulsewidth is changed, e.g., 0.25 ms for $D_R = 5\%$. It is noted that the signal of the initial high density plasma in the temporal evolution is unchanged by D_R , i.e., the temporal ratio of the high density to the steady-state phases is increased by decreasing the duty ratio. The thrust-to-power ratio is found to be increased by decreasing the duty ratio from ~ 5 mN/kW in the continuous operation to ~ 9 mN/kW for $D_R \sim 5\%$. In other words, it is experimentally demonstrated that the neutral depletion induces the decrease in the thrust-to-power ratio. Not to waste the propellant for the pulsed operation, pulsing the gas is one of the options to improve the performance.

In summary, at the initial phase of the discharge, the high plasma density is obtained inside the source and then the high density plasma exhausted from the source is detected downstream of the source after the temporal delay. Once the neutrals inside the source are depleted by the ionization process, the axial location giving the maximum plasma density is shifted to the upstream side of the source and the plasma density exhausted from the source is also decreased. It is demonstrated that the neutral-depletion-induced asymmetric density profile causes the decrease in the thrust-to-power ratio, which can be improved by using only the initial phase of the discharge.

The authors would like to thank Professor A. Fruchtman for fruitful discussions. This work is partially supported by grants-in-aid for scientific research (B 25287150 and No. A 26247096) from the Japan Society for the Promotion of Science and the Yazaki Memorial Foundation for Science and Technology.

- ¹C. Charles, *Plasma Sources Sci. Technol.* **16**, R1 (2007); and references therein.
- ²I. A. Biloiu, E. E. Scime, and C. Biloiu, *Appl. Phys. Lett.* **92**, 191502 (2008).
- ³S. Pottinger, V. Lappas, C. Charles, and R. Boswell, *J. Phys. D: Appl. Phys.* **44**, 235201 (2011).
- ⁴K. Takahashi, T. Lafleur, C. Charles, P. Alexander, R. W. Boswell, M. Perren, R. Laine, S. Pottinger, V. Lappas, T. Harle, and D. Lamprou, *Appl. Phys. Lett.* **98**, 141503 (2011).
- ⁵L. T. Williams and M. L. Walker, *J. Propul. Power* **29**, 520 (2013).
- ⁶A. Shabshelowitz and A. D. Gallimore, *J. Propul. Power* **29**, 919 (2013).
- ⁷C. Charles, K. Takahashi, and R. W. Boswell, *Appl. Phys. Lett.* **100**, 113504 (2012).
- ⁸K. Takahashi, A. Komuro, and A. Ando, *Plasma Sources Sci. Technol.* **24**, 055004 (2015).
- ⁹K. Takahashi, T. Lafleur, C. Charles, P. Alexander, and R. W. Boswell, *Phys. Rev. Lett.* **107**, 235001 (2011).
- ¹⁰A. Fruchtman, *Phys. Rev. Lett.* **96**, 065002 (2006).
- ¹¹K. Takahashi, C. Charles, and R. W. Boswell, *Phys. Rev. Lett.* **110**, 195003 (2013).
- ¹²R. W. Boswell and F. F. Chen, *IEEE Trans. Plasma Sci.* **25**, 1229 (1997); and references therein.
- ¹³A. Aanesland, L. Liard, G. Leray, J. Jolly, and P. Chabert, *Appl. Phys. Lett.* **91**, 121502 (2007).
- ¹⁴M. Shimada, G. R. Tynan, and R. Cattolica, *Plasma Sources Sci. Technol.* **16**, 193 (2007).
- ¹⁵A. M. Keesee and E. E. Scime, *Plasma Sources Sci. Technol.* **16**, 742 (2007).
- ¹⁶D. O'Connell, T. Gans, D. L. Crintea, U. Czarnetzki, and N. Sadeghi, *J. Phys. D: Appl. Phys.* **41**, 035208 (2008).
- ¹⁷C. M. Denning, M. Wiebold, and J. E. Scharer, *Phys. Plasmas* **15**, 072115 (2008).
- ¹⁸R. M. Magee, M. E. Galante, J. Carr, Jr., G. Lusk, D. W. McCarren, and E. E. Scime, *Phys. Plasmas* **20**, 123511 (2013).
- ¹⁹A. W. Degeling, T. E. Sheridan, and R. W. Boswell, *Phys. Plasmas* **6**, 3664 (1999).
- ²⁰A. Okamoto, K. Hara, K. Nagaoka, S. Yoshimura, J. Vranješ, M. Kono, and M. Y. Tanaka, *Phys. Plasmas* **10**, 2211 (2003).
- ²¹A. Fruchtman, G. Makrinich, P. Chabert, and J. M. Rax, *Phys. Rev. Lett.* **95**, 115002 (2005).
- ²²A. Fruchtman, *IEEE Trans. Plasma Sci.* **36**, 403 (2008).
- ²³E. Ahedo and J. Navarro-Cavallé, *Phys. Plasmas* **20**, 043512 (2013).
- ²⁴K. Takahashi, A. Chiba, A. Komuro, and A. Ando, *Phys. Rev. Lett.* **114**, 195001 (2015).
- ²⁵Y. Takao and K. Takahashi, *Phys. Plasmas* **22**, 113509 (2015).
- ²⁶K. Takahashi, *Rev. Sci. Instrum.* **83**, 083508 (2012).
- ²⁷P.-W. Lee and H.-Y. Chang, *Phys. Lett. A* **213**, 186 (1996).
- ²⁸S. Yoshimura, A. Okamoto, and M. Y. Tanaka, *J. Plasma Fusion Res. Ser.* **6**, 610 (2004).
- ²⁹C. Charles, R. W. Boswell, and K. Takahashi, *Plasma Phys. Controlled Fusion* **54**, 124021 (2012).